JACS
JOURNAL OF THE AMERICAN CHEMICAL SOCIETY
Article
pubs.acs.org/JACS

Determining the TiO_2-Photocatalytic Aryl-Ring-Opening Mechanism in Aqueous Solution Using Oxygen-18 Labeled O_2 and H_2O

Xibin Pang, Wei Chang, Chuncheng Chen, Hongwei Ji, Wanhong Ma,* and Jincai Zhao*

Beijing National Laboratory for Molecular Sciences, Key Laboratory of Photochemistry, Institute of Chemistry, The Chinese Academy of Sciences, Beijing 100190, China

Supporting Information

ABSTRACT: The molecules O_2 and H_2O dominate the cleavage of aromatic sp^2 C−C bonds, a crucial step in the degradation of aromatic pollutants in aqueous TiO_2 photocatalysis, but their precise roles in this process have remained elusive. This can be attributed to the complex oxidative species involved and to a lack of available models for reactions with a high yield of direct products. Here, we used oxygen-18 isotope labeled O_2 and H_2O to observe the aromatic ring-opening reaction of the model compound 3,5-di-*tert*-butylcatechol (DTBC), which was mediated by TiO_2 photocatalysis in an aqueous acetonitrile solution. By analyzing the primary intermediate products (~75% yield), especially the seven-membered ring anhydrides that were formed, we obtained direct evidence for the oxygen atom of dioxygen insertion into a C−C bond of the aromatic ring. This indicates that molecular oxygen is the ultimate ring-opening agent in TiO_2 photocatalysis and that it undergoes single O atom incorporation rather than the previously proposed molecular oxygen 1,2-addition processes. The ratio of intradiol to extradiol products depends on the particle size of TiO_2 catalysts used, which suggests that the O_2 activation is correlated with the available coordination sites on the TiO_2 surface in the photocatalytic cleavage of the aromatic ring.

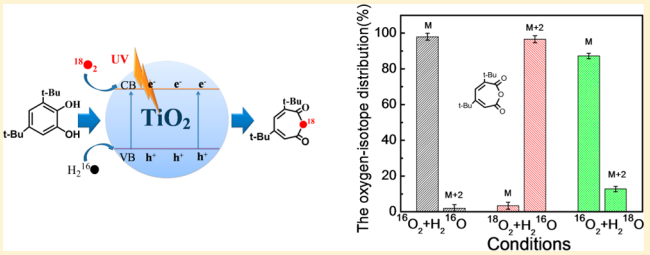

INTRODUCTION

A majority of persistent organic pollutants, such as chlorophenols (CPs), polycyclic aromatic hydrocarbons (PAHs), polychlorinated biphenyls (PCBs), dioxins, dichlorodiphenyltrichloroethane (DDT), and polybrominated diphenyl ethers (PBDEs), contain one or multiple aromatic ring structures.[1] Converting these aromatics into acyclic compounds, which are more easily metabolized and less toxic, is the key step not only in biodegradation but also in oxidative treatment technologies, such as TiO_2 photocatalytic degradation.[2] In nature, molecular oxygen usually and sometimes exclusively breaks aromatic rings catalyzed by oxygenases, such as catechol dioxygenase.[3] Two pathways for ring cleavage of catechols by dioxygenase have been classified as the intradiol and the extradiol cleavage of the ring according to the position of the broken C−C bond, namely, the intra- or the extra-1,2-dihydroxyl substituent (eq 1).

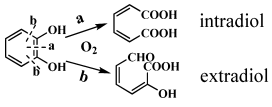

(1)

Many synthetic iron-centered complexes mimicking oxygenases have also been demonstrated to be able to catalyze dioxygen insertion into the aromatic ring.[4−7] However, there are ongoing debates on the aromatic-ring scission mechanism by advanced oxidation processes (AOPs), such as TiO_2 photocatalysis, since it was first utilized for the degradation of organic pollutants in water.[2] Unlike homogeneous enzymatic catalysis using dioxygen or thermal-catalytic reactions using a distinct oxidant, such as $KMnO_4$, ClO_2, O_3, $^1O_2$, or H_2O_2,[8] the initial reaction "reagents" of TiO_2 photocatalysis are h^+_{vb} and e^-_{cb}. The hydroxyl radical (·OH), superoxide radical ($O_2{\cdot}^-$), or hydroperoxyl radical (·OOH) species are the products of the solvent H_2O and the dissolved dioxygen reacting with h^+_{vb} and e^-_{cb}, respectively. Among them, the hydroxyl radical is believed to be the main active oxygen species (AOS)[9−11] and thought to play a key role in the entire process of the substrate degradation, which can oxidize almost all of the organic compounds to CO_2 and inorganic ions in theory (its potential is approximately 2.7 V vs NHE).[10] Corresponding to the active hydroxyl radical reactions, the oxidation process of molecular oxygen participating in TiO_2 photocatalysis is very complex.[12−21] Because of the obligatory symmetry of the spin states, the molecular oxygen species have been assumed to have numerous paradoxical ways of participating in the oxidation of organic compounds.[22] In certain cases, it has been detected in TiO_2 photocatalysis, for example, as O_2^-/·OOH activated by the molecular oxygen capturing an electron in the conduction band, as singlet $^1O_2$ via energy transfer,[23] or as dioxygen reacting with the generated carbon-centered radicals (R·) to form organic super- or peroxides.[21,24] However, it is difficult to correlate these forms with insertion into the C−C bonds of the

Received: March 31, 2014
Published: May 21, 2014

dx.doi.org/10.1021/ja5031936 | J. Am. Chem. Soc. 2014, 136, 8714−8721

aryl ring. As for the homogeneous Russell mechanism,[24] Criegge rearrangement elucidated the formation of quadruple-oxetane intermediates (ROOOOR), followed by a homolytic scission of alkyl C−C bond by inserting the oxygen of O_2 into the C−C bonds. Similarly, in the ring-opening step, the most recognized mechanism for TiO_2 photocatalysis is assumed by diverse reports to be eq 2:[14,15,25−27]

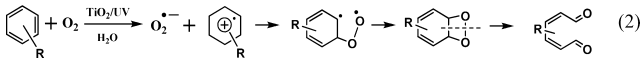

(2)

However, there is direct evidence against this proposal: for all initially aromatic substrates, the observed ring-opening products in water in the presence of dioxygen are always carboxylic acids or carboxylic acid derivatives instead of the expected dialdehyde.[14,15,28] Regarding the aromatic ring-opening process via the scission of dioxetane, aldehyde is believed to be an unstable intermediate that quickly converts to a stable carboxylic acid. Obviously, even when O_2 or H_2O is labeled with the oxygen-18 isotope, it is impossible to determine the oxygen source because the aldehyde oxygen easily exchanges its oxygen with solvent H_2O.[12,29] Other reports have recently confirmed that hydroxylation is the prerequisite for the aromatic ring cleavage, as shown in eq 3,[10,30] which directly generates the monocarboxylic or

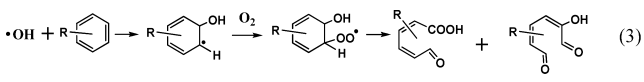

(3)

dicarboxylic acid products. It is widely agreed that a polyhydroxylated aromatic ring is more easily opened, but it is difficult to identify the oxygen source in the final acid products because of the influence of the hydroxylation originating from H_2O activation.

Recently, several groups,[18,31−33] including our group,[12,34] have demonstrated that the initial reaction between O_2 and the surficial Ti sites of TiO_2 may form *end-on* TiOOH and a *side-on* structure. The Raman spectra indicated that these species on the surface of TiO_2 originate from dioxygen in ^{18}O isotope-labeling experiments. However, these data only indicated the phenomenon that an O atom from the O_2 molecule is involved in an intermediate product (i.e., alcohol→ aldehyde[12]) rather than the cleavage of the aromatic ring. Moreover, these reactions are mostly performed in organic solvents, which cannot reflect the possibly competitive reaction of ·OH/H_2O. It is worth noting that Matsumura and co-workers[29] observed that, on anatase and rutile TiO_2, 10−30% and 60−80%, respectively, of the O atoms incorporated into the phenol were from O_2 (in competition with H_2O) during the TiO_2-photocatalytic hydroxylation of benzene in water by using isotope-labeling methods. This is the first valuable evidence for dioxygen interacting with the organic substrate in aqueous TiO_2 photocatalysis. Before this, the dioxygen was always believed to play the main role to capture the electrons in the conduction band of TiO_2 to form H_2O or H_2O_2 and hence to depress the recombination of photogenerated h^+_{vb}/e^-_{cb} pairs. Even if there is the argument that the dioxygen was incorporated into the organic molecule, it is difficult to make a distinction between

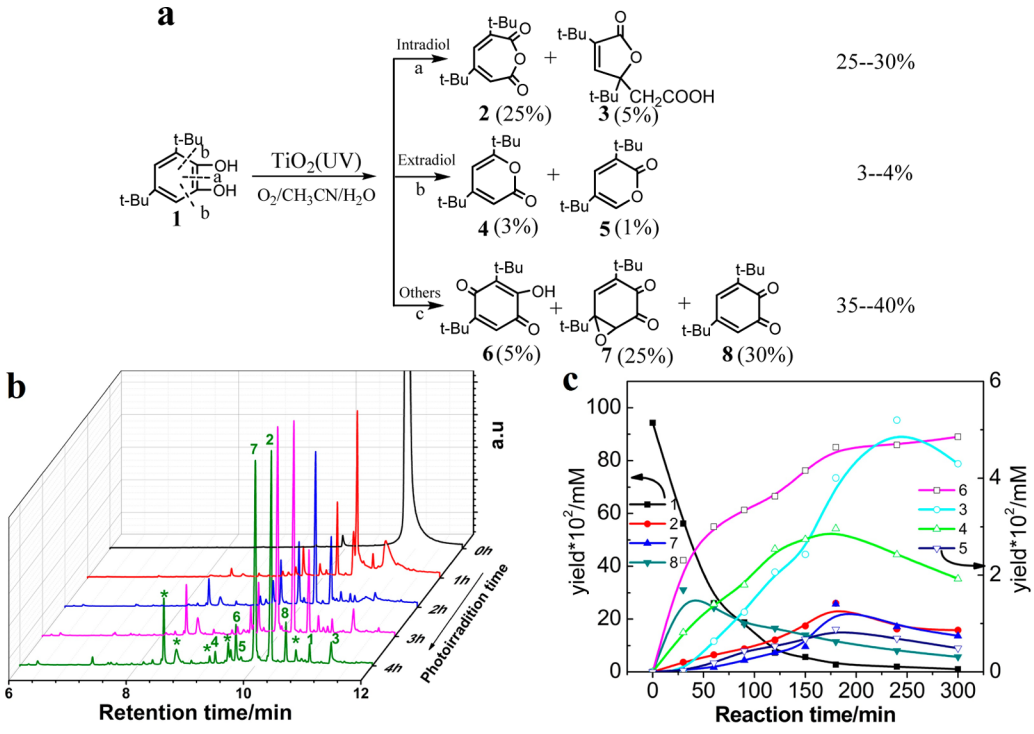

Figure 1. Structures and reaction process of the main intermediate products. (a) Several of the main products were summarized and divided into three groups; the numbers under the molecular structures correspond to the peak numbers in the chromatograms, and the figures in brackets indicate their highest yields. (b) The GC chromatograms obtained at various photoirradition times in the photo-oxidation of 3,5-di-*tert*-butylcatechol (DTBC). (c) The time evolution of the degradation of DTBC. The * symbol represents the unidentified products that are not the initial ring-opening products. The photocatalytic reactions were performed in a 25 mL closed Pyrex glass bottle containing 100 mg of TiO_2 powder (P25), 2.22 mg of DTBC, and 10 mL of water/acetonitrile (v/v = 1:1) mixed solvent (acetonitrile is used to increase the solubility of the substrate) under 1 atm of oxygen pressure or air atmosphere by a 100 W high-pressure Hg lamp.

dx.doi.org/10.1021/ja5031936 | J. Am. Chem. Soc. 2014, 136, 8714−8721

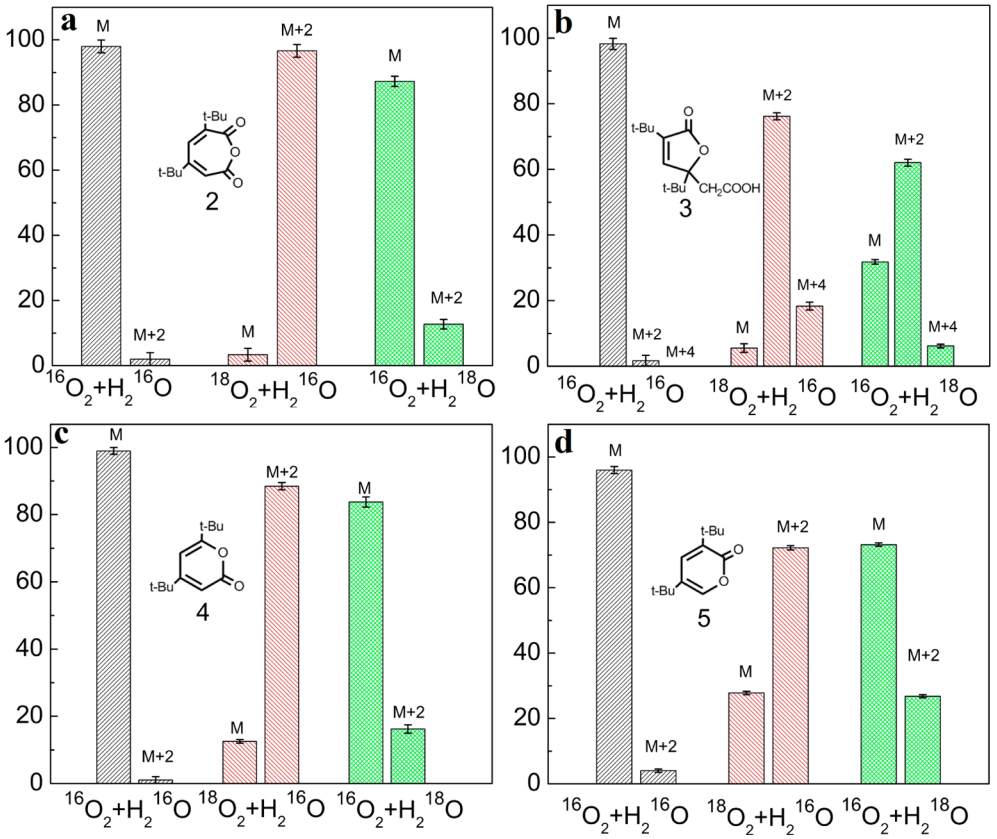

Figure 2. Oxygen-isotope distribution of the four initial ring-opening products under the various isotope conditions. (a) Product **2**; (b) product **3**; (c) product **4**; (d) product **5**. In each panel, the horizontal axis represents the three isotope conditions: (1) natural O_2 and H_2O; (2) $^{18}O_2$ and H_2O; (3) O_2 and $H_2{}^{18}O$; the vertical axis represents the oxygen-isotope distribution ratio (%); M, M + 2, and M + 4 denote products including 0, 1, and 2 atoms, respectively, of ^{18}O in place of ^{16}O.

the dioxygen and the oxygen of H_2O or between the dioxygen and the surface oxygen of TiO_2 because of the ubiquitous oxygen isotopic exchange.[35−39] In fact, our recent oxygen-18 isotope-labeling studies[20] showed that the dominant O_2-incorporating pathway in the TiO_2-photocatalytic hydroxylation of aromatics was actually through the reduction of O_2 by e^-_{cb} and the subsequent formation of free ·OH via H_2O_2. Due to the quick exchange of the oxygen isotope between the water and specific aromatic ring-opening products, such as aldehydes and the auto-oxidative product quinone, it is a great challenge to use $^{18}O_2$ or $H_2{}^{18}O$ isotope-labeling experiments to distinguish the O atom origin in the ring-opening products in aqueous TiO_2 photocatalysis. In addition, the yield of the ring-opening products for aromatic substrates is generally less than 1%,[28] which makes the investigation of their oxygen sources less significant.

Among the numerous catechol substrates used for catechol oxygenases and their synthetic iron-containing analogues, 3,5-di-*tert*-butylcatechol (DTBC) is the most widely used molecular probe because its bulky *t*-butyl groups induce the primary ring-opening reaction with unexpectedly high yields.[40−42] Moreover, its *ortho*-dihydroxyl unit ensures that the initial intradiol product is an anhydride or a dicarboxyl acid, the oxygen of which is impossible to exchange with that of H_2O. Therefore, in this work, DTBC is employed as a suitable candidate to investigate its aromatic ring-opening behaviors, even in the aqueous TiO_2-photocatalytic system where the h^+_{vb}/e^-_{cb} pair acts as "*initial reactants*". With detailed analysis of oxygen in the ring-opening products of DTBC under oxygen-18 labeling of H_2O or O_2 conditions, we are attempting to clarify whether dioxygen or H_2O is the oxygen source in breaking C−C bond of aromatic ring.

RESULTS AND DISCUSSION

Identifications of the Main Intermediate Products. To determine the highest yield of intermediate products, small aliquots of the solution were periodically sampled during the TiO_2 (P25) photocatalytic reaction and were analyzed by gas chromatography (GC) and gas chromatography−mass spectrometry (GC-MS). After optimization of the reaction conditions (see the Experimental Section), the yield of the identified products could reach nearly 75%. The gas chromatogram obtained at various times is shown in Figure 1b. For accurate quantification, a series of identical reactions were performed to yield enough intermediates to obtain their ^1H NMR data (Table S1, Supporting Information, shows the MS and ^1H NMR data of the main intermediates). The main peaks in the chromatogram are summarized in Figure 1a, including a comparison between the literature data[4,43] and the authentic compound data. Moreover, the contents of these intermediates were quantified by GC at various conversion yields (Figure 1c). Figure 1c shows that certain intermediates first increased and then decreased but the total identified yield remained greater than 70%, which indicates that most of the intermediates were involved in the main reaction of the photocatalysis of DTBC.

Among these intermediates, products **2**−**5** were the ring-opening products, and **6**−**8** were auto-oxidation products of the DTBC in which no aromatic C−C bond was completely

dx.doi.org/10.1021/ja5031936 | J. Am. Chem. Soc. 2014, 136, 8714−8721

broken. Then, we focused on the former ring-opening products **2**−**5**, in which **2** and **3** were the primary ring-opening products without the loss of a carbon atom, and they were generally intradiol products, which means that the O atom was inserted into the middle of the *ortho*-hydroxyl. Products **4** and **5** had one less carbon than their matrix and were generally extradiol products because the O atom was inserted into the outside of the two hydroxyls.[3] The yield of intradiol products was 5 times higher than that of extradiol products throughout the reaction period. The formation of intradiol products or extradiol products has been widely used to distinguish the activating ways of dioxygen in the homogeneous and biomimetic systems,[5] but this is the first time it was used in a heterogeneous photocatalytic system. More importantly, in the identified yield of ∼75%, the ring-opening products accounted for 25−30%. Compared to the results of previous aqueous TiO_2-photocatalytic reports in which the yields of the ring-opening products have always been very low (<1%), these yields are high enough to conveniently determine the oxygen sources and accurately quantify the ring-opening products by oxygen-18 isotope-labeling experiments. In addition, the GC showed that there were some other unidentified products (∼25% yield in terms of the total yield) that have less carbon numbers than the initial DTBC (according the MS data). They were not analyzed by the isotope experiments because they were not the initial ring-opening products and their oxygen atoms might come from other multiple pathways such as the ·OH radical attack, the hydrolysis, or the auto-oxidation by dioxygen.

^{18}O Isotope-Labeling Studies. For each of the several possible pathways mentioned for ring opening, the participation of the solvent H_2O is indispensable, despite the fact that the hydroxyl radicals are derived from water oxidation by holes or direct oxidation by holes with further hydrolysis. Because water cannot be involved in the same way as dioxygen or related species, that is, oxidative cleavage of the aromatic ring via homolysis of the dioxetane intermediate, quantification of the oxygen source of the initial ring-opening products **2**−**5** is the most direct evidence to show whether ·OH/H_2O or dioxygen ultimately opens the aromatic rings. In the present work, the photocatalytic ring-opening reactions of DTBC were performed using labeled $^{18}O_2$ (purity, >97%)/$H_2{}^{16}O$ and $^{16}O_2$/$H_2{}^{18}O$ (purity, 98%), respectively. The isotope abundance of the products for each sample was analyzed by GC-MS at various conversion yields (Figure S2, Supporting Information). The fragmentation patterns were compared with those of the products obtained by the reaction under the natural isotope abundances of $^{16}O_2$ and $H_2{}^{16}O$. Figure 2 shows the isotope abundance of the initial ring-opening products **2**−**5** at a conversion yield of 95%. The products **2**, **4**, and **5**, including the isotope abundance of M and M + 2, indicated that they only incorporated one labeled oxygen atom, whereas product **3** contains the isotope peaks of M + 2 and M + 4, which means that there were one and two labeled oxygen atoms incorporated into the products, respectively.

The yield of product **2** was the highest among all of the cleavage products (∼25% yield). For $^{18}O_2/H_2{}^{16}O$ (Figure 2a, middle), nearly the entire inserted oxygen atom in the ring (M + 2 > 98%) was derived from $^{18}O_2$, whereas only less than 1% (M + 2) (Figure 2a, left) was for $^{16}O_2/H_2{}^{16}O$ in the controlled experiment, which was further confirmed by electrospray ionization mass spectrometry (ESI-MS) (Figure S8, Supporting Information). In addition, in the whole reaction period, the isotopic profile of product **2** at every reaction stage maintained the same ratio (∼98%) in the $^{18}O_2/H_2{}^{16}O$ case (Figure S2, Supporting Information). Such a high and stable oxygen-isotope distribution in **2** also indicates that 18-oxygen of product **2** would neither exchange with the oxygen of H_2O nor the surface oxygen of TiO_2 in this system. The entire inserted oxygen atom of product **2** from O_2 is the most direct evidence for the O_2 splitting an aromatic ring in the photocatalytic reaction. This implies the single-oxygen insertion, rather than the insertion of both oxygen atoms of the O_2 that remained in the products, which is different from the results in previous reports. Namely, although the oxidative power of both h_{vb}^+ and the ·OH radical are stronger than that of the O_2 in TiO_2 photocatalysis, only O_2 can insert one of its oxygen atoms into the C−C bond of the aromatic ring to form intradiol product **2**.

When the reaction was performed in ^{18}O-enriched water ($H_2{}^{18}O$) using $^{16}O_2$ in air as the oxidant ($^{16}O_2/H_2{}^{18}O$), the ^{16}O isotope from the dioxygen (Figure 2a, right) did not achieve the same abundance of ∼98% as observed for the $^{18}O_2/H_2{}^{16}O$ case; only 88% was observed. Specifically, ∼10% of the inserted O atoms came from the solvent $H_2{}^{18}O$, and the majority derived from $^{16}O_2$. Does this mean that a small part of the ring breakage is actually achieved via H_2O activation and insertion, for example, by holes directly oxidizing H_2O into ·OH radicals or by organic radical cation ($R^{+\cdot}$) hydrolysis (the hydroxylation of the ring)? To clarify if the 10% oxygen originated from H_2O, we performed the following experiments to investigate the possible role of H_2O in the ring-opening reaction.

First, the exchange of the ^{16}O atoms in both the reactant DTBC and the product **2** with $H_2{}^{18}O$ or $^{18}O_2$ in the reaction was slow and can be ignored under the present experimental conditions (Figure S3, Supporting Information), and hence, it is reasonable to believe that the intermediates underwent the exchange of oxygen with H_2O before the final products formed. Among the intermediates of **6**−**8** before the ring opened, the most possible origin was that a part of the auto-oxidation intermediate quinone **8** exchanges oxygen with $H_2{}^{18}O$ and then these ^{18}O-containing quinones were photocatalytically decomposed to form the product **2**, as shown in eq 4:

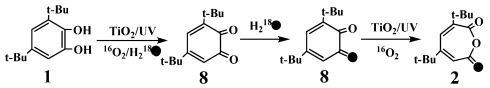

(4)

Thus, we performed the isotopic-exchange experiment of quinone **8** with $H_2{}^{18}O$ in the dark reaction (Figure S7, Supporting Information). The results indicated that the ^{16}O of quinone **8** exchanged one of its O atoms with $H_2{}^{18}O$ even in the dark reaction (45% exchanged in 3 h) and then was converted into the product **2** by TiO_2 when irradiated by UV light. Specifically, 8−10% oxygen from H_2O in product **2** for the $^{16}O_2/H_2{}^{18}O$ reaction media underwent oxygen exchange with $H_2{}^{18}O$ before the ring-opening reaction, not that $H_2{}^{18}O$ led to the ring-opening reaction. However, such a circumstance could not be observed in the $^{18}O_2/H_2{}^{16}O$ case because there is not any difference between the oxygen in the substrate DTBC or **8** and in H_2O (in both cases, the oxygen was ^{16}O). So whether in the $^{18}O_2/H_2{}^{16}O$ or $^{16}O_2/H_2{}^{18}O$ case, the inserted O atoms of the product **2** all result from O_2.

This conclusion was further confirmed by the formation of the extradiol products **4** and **5** (Figure 2c, d). Despite their low yield (total ∼4%), products **4** and **5** have already been proven in enzymatic catalysis reactions to be the products of the

dx.doi.org/10.1021/ja5031936 | J. Am. Chem. Soc. 2014, 136, 8714−8721

extradiol product lactone with a further loss of the carbonyl group.[5,44,45] Figure 2c, d showed that there were 85% and 75% of the inserted O atoms of products **4** and **5**, respectively, from O_2 for the $^{18}O_2$/ $H_2{}^{16}O$ condition. Such a high percentage of H_2O involved in the formation of products **4** (15%) and **5** (25%) relative to that of **2** was due to the unavoidable, reversible hydrolysis reaction of the lactone compound and the following exchange with H_2O between its α-ketone oxygen, which has been confirmed in homogeneous, enzymatic catalytic systems (Figure S9, Supporting Information).[44]

When the experimental conditions changed to $^{16}O_2/H_2{}^{18}O$, the same trend of the dioxygen insertion in the $^{18}O_2/H_2{}^{16}O$ case was observed, in which the majority of the inserted O atoms came from dioxygen (Figure 2c, d). The isotopic-exchange experiments of products **4** and **5** showed that they could not exchange the O atom with O_2 or H_2O during the reaction (Figures S5 and S6, Supporting Information). Now, all of the initial oxygen sources of products **2**, **4**, and **5** (before exchange with H_2O) resulted from the insertion of one oxygen atom of the dioxygen, which was significantly different from the hydroxylation of the aromatic ring,[20,29] decarboxylation of the acids,[21] and other C−H or C−C bond oxidations involved in the O_2/H_2O media in which the dominant oxygen source of the products was H_2O. This labeling oxygen result confirmed for the first time the hypothesis that the dioxygen exclusively breaks an aromatic ring in aqueous TiO_2 photocatalysis.

The most interesting finding is the formation of product **3**, for which it has been widely shown that product **2** was the precursor for all of the homogeneous ring-opening systems. To investigate whether it also occurs in the TiO_2 photocatalysis, a control trial was performed. Product **2** was isolated and deliberately hydrolyzed by an acid and an alkali and by reacting under photocatalytic conditions, respectively. We always obtained product **3** instead of muconic acid for both photocatalysis and acid−base catalysis (Figure S8, Supporting Information). Even if the oxygen in product **2** was derived entirely from the dioxygen, there was no M or M + 4 in product **3** for $^{18}O_2/H_2{}^{16}O$ or $^{16}O_2/H_2{}^{18}O$, and the M + 2 peak should be nearly 100% of oxygen profile, according to the hydrolysis reaction (eq 5a). However, for the $^{18}O_2/H_2{}^{16}O$ reaction media,

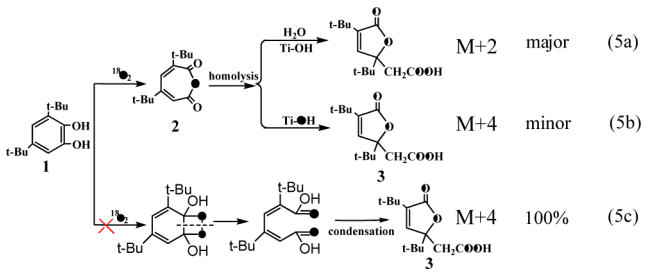

both one ^{18}O atom (M + 2 of ∼77%) and two ^{18}O atoms (M + 4 of ∼18%) existed in **3** (Figure 2b, middle). This demonstrated that the majority of product **3** resulted from the hydrolysis reaction of product **2** (∼77%) and that a component of two-oxygen atom addition from dioxygen (18%) also exists. This clearly means that the addition process of the second oxygen of product **2** may be from hydrolysis, too. However, it substituted with the "H_2O" that in another oxygen atom remained on the nearest surface Ti sites from O_2 to form product **3**. The high percentage of the M peak (∼31%) for $^{16}O_2/H_2{}^{18}O$ (Figure 2b, right) also suggested that the formation of product **3** could proceed by a stepwise one-oxygen atom of dioxygen insertion via the intermediate product **2**, which is then immediately hydrolyzed by the nearest Ti−OH formed from the splitting of O_2 on the surface (eq 5b) rather than by a dioxetane intermediate (eq 5c). If the reaction proceeded according to eq 5c, the M + 4 profile in **3** should be 100% or at least dominate for $^{18}O_2/H_2{}^{16}O$.

The oxygen-isotope distribution of the four initial ring-opening products showed that, no matter how strong the oxidative capacity of ·OH/h_{vb}^+ was, it was not the main active species in the oxidative cleavage for the aromatic ring. This means that the cleavage of the sp^2 C−C bond of the aromatics was not via the traditional out-sphere oxidation by ·OH or the inner-sphere h_{vb}^+ in TiO_2 photocatalysis.[11] It was the molecular oxygen that broke the sp^2 C−C bond of the aromatics. This was not preceded via a common dioxetane intermediate. It is product **2** instead of the muconic acid that is generated initially in the dioxygen insertion reaction of DTBC. No evidence for muconic acid formation could be obtained, either by high-performance liquid chromatography−electrospray ionization (HPLC-ESI) or GC-MS of the compound or of its silylated derivative. The most direct evidence to support the single oxygen insertion leading to the aromatic ring breaking was that the oxygen in product **2** was exclusively from dioxygen.

Effect of TiO_2 Particle Size on the Distribution Ratio between the Intradiol and Extradiol Ring-Opening Products. How did the active sites on the surface of the TiO_2 particles enable the single O atom of dioxygen insertion? The DTBC ring-opening products by O_2 in our system resembled in particular those in the iron(II/III) coordination catalysis. It was reminiscent of an iron-containing enzyme catalyzing DTBC with two reaction pathways, depending on the initial sites of O_2 coordination that lead to distinct intradiol or extradiol ring-opening products.[3,5,7,46] Thus, we argued that the activation and insertion of O_2 into the aromatic ring in the present case correlated to its coordination to the Ti sites on the TiO_2 surface.

A degree of coordinative unsaturation was generally required for heterocatalytic activity.[47] Figure 3a showed the defects on the surface of TiO_2, for which the Ti sites on the terrace were generally 5-fold coordinated (Ti-5c), these on the edges and steps were Ti-4c, and those on the corners or partly oxygen vacancies were Ti-3c.[47−49] The sites at edges, steps, corners, or oxygen vacancies had a sufficient number of dangling bonds to coordinate to either the dissociative catechol or the O_2 in place of solvent H_2O, whereas the terrace sites (Ti-5c) could not form the five-membered ring of the charge-transfer complex of DTBC.[49,50] The most important difference between Ti-4c and Ti-3c sites, after coordinating to DTBC, was that the latter left an unoccupied site that may coordinate to O_2 and undergo reductive activation with photoinduced $Ti^{3+}(e_{cb}^-)$, while the former had to activate O_2 via the attack of DTBC radical intermediate (mediated by h_{vb}^+) (Figure 4).

Generally, the particle size of TiO_2 affects the distributions of Ti coordination sites on the surface. Additionally, the smaller the particle size is, the greater the number of defects, and the more Ti-4c and Ti-3c circumstances present.[51] Rajh and co-workers[52] used X-ray absorption near-edge spectroscopy (XANES) studies to show a decrease in the coordination number of the surface Ti sites with decreasing particle size, and extended X-ray absorption fine structure (EXAFS) results demonstrated that the small particles converted surface sites into more reactive "*corner defects*". So, we selected several TiO_2 particle samples with different size (Figure S10, Supporting

dx.doi.org/10.1021/ja5031936 | J. Am. Chem. Soc. 2014, 136, 8714−8721

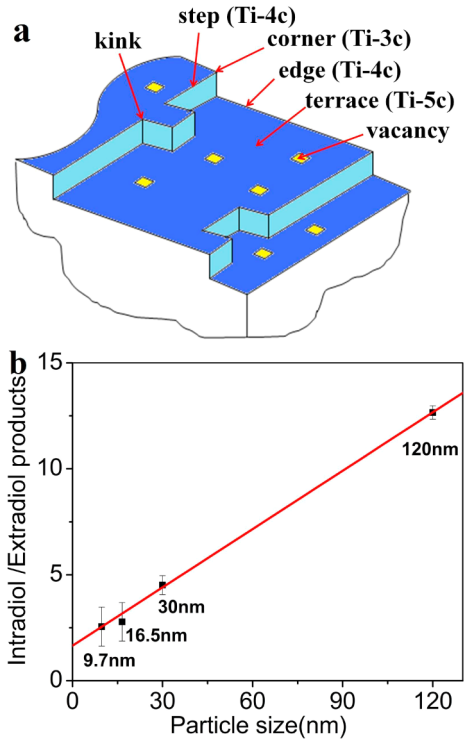

Figure 3. Correlation between the particle size and the ratio of intradiol to extradiol ring-opening products. (a) Schematic diagram for various types of coordinate sites on the surface of TiO_2. (b) Relationship between the TiO_2 particle size and the ratio of intradiol to extradiol ring-opening products.

Information) to observe the changes in the ratio of the intradiol to extradiol products. These TiO_2 particles have identical crystal structures (Figure S11, Supporting Information) and similar defect concentrations in bulk, as measured by our positron annihilation experiments (Table S3, Supporting Information), but different exposed Ti-site coordination on the surface. Our experiment results (Figure 3b) showed that the ratio of the intradiol to extradiol products was indeed nearly linear with the particle size of the TiO_2 samples. Although the overall photocatalytic reaction rate of DTBC significantly slowed down with the increase in the TiO_2 particle size, the ratio of intradiol to extrdiol products still increased linearly.

Given that the exclusive O_2 insertion generates intradiol and extradiol products as discussed above, this primary result indicated that the manner of O_2 activation and participation into ring opening was correlated to the coordinating properties of TiO_2 surface sites that were geometrical size dependent. In geometry, the terraces (main Ti-5c) had the highest proportion, the steps (Ti-4c) or kinks were in the middle, and the corners (Ti-3c) were the least prevalent for any crystal. The sites on the terraces that could not form the five-membered ring complex with DTBC generally have little activity and may only be correspond to the auto-oxidation products or other unknown deeper oxidation (Figure 4a). The most noteworthy was that, even for the smallest size of TiO_2 particles (~9.7 nm), the intradiol products were still more than extradiol products (the ratio was about 2.5, Figure 3 b). This was well consistent with the geometrical proportions of Ti-4c and Ti-3c sites on the surface of any size of TiO_2 nanocrystals. If the participation of O_2 in the ring-opening reaction through either Ti^{3+} (or e_{cb}^-) or anchored DTBC radicals was presumed with the similar rate (both was converted into superoxide radical initially), the high proportion of the intradiol products for all four TiO_2 samples would suggest that intradiol products must be yielded on the steps (Ti-4c) or kinks, where the O_2 should be activated and incorporated by the anchored DTBC radicals, since there was no available Ti site left for O_2 coordination and reduction (Figure 4b). Similarly, a small proportion of the extradiol products should be delivered from the corners (Ti-3c) or partly oxygen vacancies (also Ti-3c) with the smallest distribution proportion on the surface, and the activation of O_2 was performed by Ti^{3+} (or e_{cb}^-) because there was an available Ti site left for O_2 coordination (Figure 4c). The distribution of the ring-opening products and the ratio of the corresponding Ti sites on the surface of the TiO_2 matched very well. Even if there

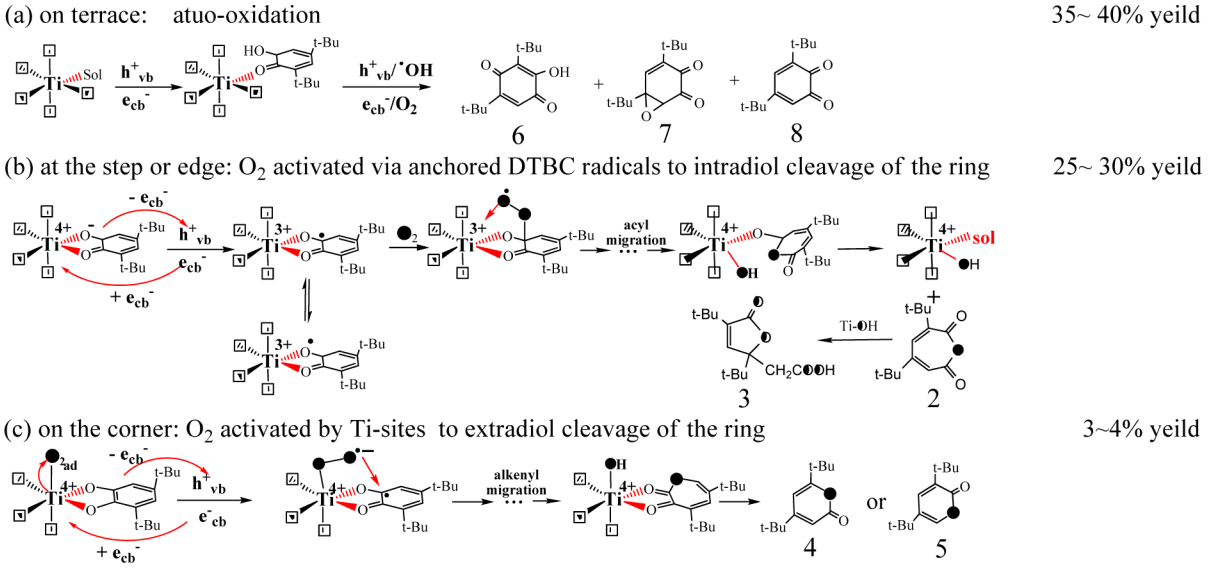

Figure 4. Proposed mechanism for singly O atom incorporation in the photocatalytic cleavage of DTBC by TiO_2. (a) Auto-oxidation by $\cdot OH/h_{vb}^+$ on terrace, (b) intradiol cleavage via the anchored DTBC radicals active dioxygen at the step or edge, (c) extradiol cleavage via Ti-site active dioxygen on the corner.

dx.doi.org/10.1021/ja5031936 | J. Am. Chem. Soc. 2014, 136, 8714−8721

existed another pathway such as photosensitized redox reaction via excitation of the surface CT complex of DTBC−Ti sites to convert the O_2 into superoxide radical anion and DTBC into radical cation, respectively, the ultimately DTBC ring-opening steps by O_2 must take place via the coordination of the O_2 or DTBC with the Ti site on the surface as the paths in Figure 4b or c. Otherwise, the reaction between separate DTBC radical cation and superoxide radical anion without Ti coordination should be only through the dioxetane intermediate as described in eq 2 to generate double oxygen insertion product. However, all of our isotopic-labeling results did not support the insertion of two oxygen atoms. This suggested that there might be two different pathways of dioxygen activation depending on the available coordination number of the surficial Ti sites in the photocatalytic cleavage of the aromatic ring. Of course, it was far from establishing the distinct structure−property relationship only by means of the particle size correlation with the ratio of intradiol to extradiol products, and we expected to provide more direct evidence to support this proposed mechanism in future studies.

In conclusion, we studied the TiO_2-photocatalytic splitting aromatic ring of DTBC in aqueous acetonitrile solution and identified the main ring-opening intermediate products. Our ^{18}O isotope-labeling experimental results provided direct evidence that molecular oxygen was the sole ring-opening oxidant and nearly all of the oxygen inserted for either the intradiol or extradiol products came from a single O atom of O_2. This was interpreted as a single O atom incorporation mechanism rather than the mechanism via the dioxetane intermediate in the aromatic C−C cleavage. Two types of ring cleavage, intradiol and extradiol by insertion of dioxygen, were determined and probably linked to the coordination environment of the surficial Ti sites of the TiO_2 photocatalyst. The role of dioxygen activation we proposed here for the TiO_2-photocatalyic degradation of DTBC in water should be taken into account for other aromatics and accordingly should be considered to improve the efficiency of TiO_2 photocatalysis for water purification.

EXPERIMENTAL SECTION

Materials. All reagents and solvents were purchased from commercial sources and were used without further purification, unless otherwise noted. TiO_2 powder (P25) was purchased from Degussa Co. Four samples of anatase TiO_2 nanocrystals were purchased from Aladdin Chemical Co. Each of the commercial TiO_2 samples was suspended in aerated aqueous solution and irradiated for 48 h by UV light before they were used. After the treatment, the suspended TiO_2 were separated by centrifugation, and the catalysts were further washed several times by distilled water, dried at 120 °C for 5 h, calcined at 400 °C for 3 h in air, and sealed. The molecules DTBC and 3,5-di-*tert*-butyll-o-quinone (DTBQ) were obtained from Aldrich Chemical Co. Acetonitrile was of HPLC grade, and 1,2-dichloromethane was analytical-grade. $H_2{}^{18}O$ was purchased from Jiangsu Changshu Chemical, Limited. The isotopic enrichment was 98%, determined by MS. $^{18}O_2$ was purchased from Cambridge Isotope Laboratories, Inc. The isotopic enrichment was greater than 97%. Deionized and doubly distilled water was used throughout this study.

Physical Measurements. The particle size of the anatase TiO_2 nanocrystals was confirmed on an FEI Tecnai G^2 F30 (200 kV), and the Brunauer−Emmett−Teller (BET) surface area was measured on an AUTOSDRB-1 using N_2 adsorption at −196 °C for the ceria sample predegassed at 120 °C under vacuum for 2 h. X-ray diffraction (XRD) patterns were obtained on a Bruker Advance AXS diffractometer with Cu Kα irradiation at 40 kV and 100 mA. The defects in the TiO_2 samples were characterized by positron annihilation. The positron annihilation lifetime spectra (PALS) were measured using a conventional ORTEC-583 fast-slow coincident system at room temperature. The coincidence spectrometer used had a prompt-time resolution of 196.54 ps (fwhm) for the γ-rays from a ^{60}Co source selected under the experimental conditions. The sample powder was pressed into a disk (diameter: 10.0 mm; thickness: 1.0 mm). A 30 μci ^{22}Na positron source was sandwiched between two identical sample disks. Each spectrum contained 2.0×10^6 for PATFIT. The positron lifetime spectrum containing 10^6 counts was analyzed by the PATFIT program to be decomposed into several lifetime components. The products were analyzed using an Agilent 7890A series gas chromatograph equipped with a flame ionization detector (FID) and a HP-5 capillary column (30 m × 0.25 mm × 2.5 μm). The GC-MS analysis was performed on an Agilent 7890A series gas chromatograph using an HP-5 capillary column (30 m × 0.25 mm × 2.5 μm), coupled with an Agilent 5975C (electron ionization) mass spectrometer. HPLC-ESI (APCI) was analyzed by Agilent LC 1200/ion trap 6310 with a C18 reversed-phase column (250 mm × 4.6 mm). ^1H NMR spectra were recorded on a Bruker 300 MHz ^1H NMR spectrometer.

General Procedure. The photocatalytic reactions were all performed in a 25 mL closed Pyrex glass bottle containing 100 mg of TiO_2 powder (various particle sizes), 2.22 mg of DTBC, and 10 mL of water/acetonitrile (v/v = 1:1) mixed solution in which acetonitrile is used to increase the solubility of the substrate. To equilibrate the adsorption of the substrate, the mixture was vigorously stirred for 30 min before irradiation. Then, the reaction solution was photoirradiated under 1 atm of oxygen pressure or air atmosphere by a 100 W high-pressure Hg lamp (Toshiba SHL-100UVQ) with continuous stirring by a magnetic stirrer. To trace an oxygen isotope in the products, either 98% $H_2{}^{18}O$-containing water or $^{18}O_2$ was used as the oxygen-isotope source.

Identification of the Intermediate Products. After stopping the reactions at the specified time, the suspended TiO_2 was separated by centrifugation, and then, the solution was extracted three times with 5 mL of 1,2-CH_2Cl_2. The 1,2-CH_2Cl_2 layer was then dried over anhydrous Mg_2SO_4, filtered, and rinsed three times with 5 mL of fresh 1,2-CH_2Cl_2. The combined filtrate was evaporated to dryness in vacuo at 30 °C by rotary evaporation, and the residues were then dissolved in 0.5 mL of acetonitrile or silylated[53] in 0.1 mL of anhydrous pyridine by 0.1 mL of hexamethyldisilazane and 0.05 mL of chlorotrimethylsilane before being analyzed by GC and GC-MS. To compare the samples to those described above, a run was dried by freeze-drying and then either silylated or not. The separation and purification of the main products was accomplished by column chromatography over silica gel (80−100 mesh) using 1−5% ethyl acetate in *n*-hexane, and the components were identified by the retention times of GC-MS (EI) and ^1H NMR spectroscopy. All of the products were quantified using GC (FID) with the following temperature program: injector temperature, 250 °C; initial temperature, 60 °C; hold time, 1 min, then increasing at a rate of 15 °C min^{-1} to 280 °C; and FID temperature, 280 °C. GC-MS analysis was performed under conditions identical to those used for the GC analysis.

ASSOCIATED CONTENT

Supporting Information

Degradation of DTBC under different conditions; ^1H NMR, MS data, and isotope-exchange experiments of the initial ring-opening products; transmission electron microscopy images, XRD data, BET data, electron diffraction images, and the positron annihilation lifetime of TiO_2 nanocrystals. This material is available free of charge via the Internet at http://pubs.acs.org.

AUTHOR INFORMATION

Corresponding Authors

whma@iccas.ac.cn
jczhao@iccas.ac.cn

Notes

The authors declare no competing financial interest.

■ ACKNOWLEDGMENTS

This work was supported by 973 project (nos. 2010CB933503 and 2013CB632405), NSFC (nos. 21137004, 21322701, and 21221002), and the "Strategic Priority Research Program" of the Chinese Academy of Sciences (no. XDA09030200).

■ REFERENCES

(1) Jones, K. C.; de Voogt, P. *Environ. Pollut.* **1999**, *100*, 209.
(2) *Photocatalysis and Water Purification*; Pichat, P., Ed.; Wiley-VCH: Weinheim, Germany, 2013.
(3) Costas, M.; Mehn, M. P.; Jensen, M. P.; Que, L. *Chem. Rev.* **2004**, *104*, 939.
(4) Visvaganesan, K.; Mayilmurugan, R.; Suresh, E.; Palaniandavar, M. *Inorg. Chem.* **2007**, *46*, 10294.
(5) Xin, M. T.; Bugg, T. D. H. *J. Am. Chem. Soc.* **2008**, *130*, 10422.
(6) Kovaleva, E. G.; Lipscomb, J. D. *Science* **2007**, *316*, 453.
(7) Jo, D.-H.; Que, J. L. *Angew. Chem., Int. Ed.* **2000**, *39*, 4284.
(8) Mander, L. N.; Williams, C. M. *Tetrahedron* **2003**, *59*, 1105.
(9) Hoffmann, M. R.; Martin, S. T.; Choi, W.; Bahnemann, D. W. *Chem. Rev.* **1995**, *95*, 69.
(10) Wang, J. L.; Xu, L. J. *Crit. Rev. Environ. Sci. Technol.* **2012**, *42*, 251.
(11) Dimitrijevic, N. M.; Rozhkova, E.; Rajh, T. *J. Am. Chem. Soc.* **2009**, *131*, 2893.
(12) Zhang, M.; Wang, Q.; Chen, C.; Zang, L.; Ma, W.; Zhao, J. *Angew. Chem., Int. Ed.* **2009**, *48*, 6081.
(13) Jenks, W. S. In *Photocatalysis and Water Purification*; Wiley-VCH: Weinheim, Germany, 2013; pp 25−51.
(14) Fox, M. A.; Chen, C. C.; Younathan, J. N. N. *J. Org. Chem.* **1984**, *49*, 1969.
(15) Li, X.; Cubbage, J. W.; Jenks, W. S. *J. Org. Chem.* **1999**, *64*, 8525.
(16) Lu, G.; Linsebigler, A.; Yates, J. T. *J. Phys. Chem.* **1995**, *99*, 7626.
(17) Wang, Y.; Hong, C.-S. *Water Res.* **2000**, *34*, 2791.
(18) Li, Y.-F.; L, Z.-P.; Liu, L.L.; Gao, W. *J. Am. Chem. Soc.* **2010**, *132*, 13008.
(19) Szabo-Bardos, E.; Markovics, O.; Horvath, O.; Toro, N.; Kiss, G. *Water Res.* **2011**, *45*, 1617.
(20) Li, Y.; Wen, B.; Yu, C. L.; Chen, C. C.; Ji, H. W.; Ma, W. H.; Zhao, J. C. *Chem.—Eur. J.* **2012**, *18*, 2030.
(21) Wen, B.; Li, Y.; Chen, C. C.; Ma, W. H.; Zhao, J. C. *Chem.—Eur. J.* **2010**, *16*, 11859.
(22) Daimon, T.; Hirakawa, T.; Kitazawa, M.; Suetake, J.; Nosaka, Y. *Appl. Catal., A* **2008**, *340*, 169.
(23) Daimon, T.; Nosaka, Y. *J. Phys. Chem. C* **2007**, *111*, 4420.
(24) Russell, G. A. *J. Am. Chem. Soc.* **1957**, *79*, 3871.
(25) Cermenati, L.; Albini, A.; Pichat, P.; Guillard, C. *Res. Chem. Intermed.* **2000**, *26*, 221.
(26) Chen, C.; Lei, P.; Ji, H.; Ma, W.; Zhao, J.; Hidaka, H.; Serpone, N. *Environ. Sci. Technol.* **2003**, *38*, 329.
(27) Cermenati, L.; Pichat, P.; Guillard, C.; Albini, A. *J. Phys. Chem. B* **1997**, *101*, 2650.
(28) Yang, J.; Dai, J.; Chen, C.; Zhao, J. *J. Photochem. Photobiol., A* **2009**, *208*, 66.
(29) Thuan, D. B.; Kimura, A.; Ikeda, S.; Matsumura, M. *J. Am. Chem. Soc.* **2010**, *132*, 8453.
(30) Jacob, N.; Balakrishnan, I.; Reddy, M. P. *J. Phys. Chem. C* **1977**, *81*, 17.
(31) Nakamura, R.; Imanishi, A.; Murakoshi, K.; Nakato, Y. *J. Am. Chem. Soc.* **2003**, *125*, 7443.
(32) Nakamura, R.; Nakato, Y. *J. Am. Chem. Soc.* **2004**, *126*, 1290.
(33) Nakamura, R.; Nakato, Y. *Solid State Phenom.* **2010**, *162*, 1.
(34) Wang, Q.; Zhang, M. A.; Chen, C. C.; Ma, W. H.; Zhao, J. C. *Angew. Chem., Int. Ed.* **2010**, *49*, 7976.
(35) Avdeev, V. I.; Bedilo, A. F. *J. Phys. Chem. C* **2013**, *117*, 2879.
(36) Pichat, P.; Courbon, H.; Enriquez, R.; Tan, T. T. Y.; Amal, R. *Res. Chem. Intermed.* **2007**, *33*, 239.
(37) Henderson, M. A. *J. Phys. Chem.* **1995**, *99*, 15253.
(38) Sato, S. *J. Phys. Chem.* **1987**, *91*, 2895.
(39) Courbon, H.; Formenti, M.; Pichat, P. *J. Phys. Chem.* **1977**, *81*, 550.
(40) Stitt, F.; Bailey, G. F.; Coppinger, G. B.; Campbell, T. W. *J. Am. Chem. Soc.* **1954**, *76*, 3642.
(41) Grinstead, R. R. *Biochemistry (Moscow)* **1964**, *3*, 1308.
(42) Monzani, E.; Battaini, G.; Perotti, A.; Casella, L.; Gullotti, M.; Santagostini, L.; Nardin, G.; Randaccio, L.; Geremia, S.; Zanello, P.; Opromolla, G. *Inorg. Chem.* **1999**, *38*, 5359.
(43) Weiner, H.; Finke, R. G. *J. Am. Chem. Soc.* **1999**, *121*, 9831.
(44) Funabiki, T.; Mizoguchi, A.; Sugimoto, T.; Tada, S.; Tsuji, M.; Sakamoto, H.; Yoshida, S. *J. Am. Chem. Soc.* **1986**, *108*, 2921.
(45) Lin, G.; Reid, G.; Bugg, T. D. H. *J. Am. Chem. Soc.* **2001**, *123*, 5030.
(46) Bugg, T. D. H.; Lin, G. *Chem. Commun.* **2001**, 941.
(47) Idriss, H.; Barteau, M. A. In *Advances in Catalysis, Vol 45: Impact of Surface Science on Catalysis*; Gates, B. C., Knozinger, H., Eds.; Elsevier Academic Press Inc: San Diego, CA, 2000; Vol. *45*, p 261.
(48) Farges, F.; Brown, G. E., Jr.; Rehr, J. J. *Phys. Rev. B* **1997**, *56*, 1809.
(49) Lana-Villarreal, T.; Rodes, A.; Perez, J. M.; Gomez, R. *J. Am. Chem. Soc.* **2005**, *127*, 12601.
(50) Barteau, M. A. *Chem. Rev.* **1996**, *96*, 1413.
(51) Dimitrijevic, N. M.; Saponjic, Z. V.; Rabatic, B. M.; Poluektov, O. G.; Rajh, T. *J. Phys. Chem. C* **2007**, *111*, 14597.
(52) Rajh, T.; Nedeljkovic, J. M.; Chen, L. X.; Poluektov, O.; Thurnauer, M. C. *J. Phys. Chem. B* **1999**, *103*, 3515.
(53) Sweeley, C. C.; Bentley, R.; Makita, M.; Wells, W. W. *J. Am. Chem. Soc.* **1963**, *85*, 2497.